HYSTERETIC BEHAVIOR OF STEEL BRACES SUBJECTED TO HORIZONTAL LOAD DUE TO EARTHQUAKE

by

Minoru WAKABAYASHI[I], Takeshi NAKAMURA[II], Michio SHIBATA[III]

Nozomu YOSHIDA[IV] and Hiromi MASUDA[V]

SYNOPSIS

In this paper, discussed are the elastic-plastic hysteretic behavior of steel braces which play an important role as the earthquake resistant elements of steel structures. Experimental and theoretical investigations on the braces by the authors are briefly introduced in the first half. In the latter half, idealized post-buckling curve and hysteresis loops of the brace members are formulated and proposed for the design use, based on the parametric analysis of the experimental and theoretical results.

INTRODUCTION

The earthquake resistant function of steel structures with a vertical bracing system, much depends on the hysteretic behavior of braces. It is essential to obtain the appropriately idealized restoring force characteristics and hysteretic rules of bracing members which are usefully applicable to the structural design. The elastic-plastic behaviors of simply supported steel braces under monotonic and alternately repeated loading were investigated experimentally by the authors in Refs. 1), 2), 3) and theoretically in Refs. 5), 6), 7), 8). The behaviors of braces under more realistic condition, were reported in Refs. 4), 6), 9). A parametric data analysis for the results of above-mentioned researches was performed to formulate idealized hysteresis loops for a single brace. The loops for paired braces whose behaviors do not interact each other can be obtained by the superposition method.

EXPERIMENTAL STUDIES

A series of experiments was conducted to investigate the fundamental properties of the elastic-plastic behavior of braces. In the first series, tested are simply supported bars with square cross section(15x15 mm). Figure 1 shows an example of load-displacement relationships reported at the 5th WCEE, in Rome. In the figures, n and δ are the non-dimensional expressions of the axial force N and the axial displacement Δ, respectively, divided by their yield values; Ny and Δy. n_E is the slenderness parameter defined as the ratio of Euler load N_E to Ny. Basic characteristics of a brace were obtained from this experimental study. In the second series of experiments, wide flange braces(H-50x50x6x6) in a single or double bracing system were tested under more realistic condition. Main interestings were framed effects and the effects of local instability of section elements on the hysteretic behavior. Test set-up and specimen are illustrated in Figs. 2(a) and (b), respectively. Figs. 2(c) and (d) show examples of load-displacement curves. Main informations from the test are as follows: (a) Hysteresis loops under the prescribed displacement amplitude stabilize more rapidly in the case of strong axis buckling than weak axis buckling. However, after a few cycles of loading lateral deflection becomes predominant about a weak axis. (b) The behavior of a single brace specimen designed to buckle about its weak axis in plane of the frame is almost the same as that designed to buckle out of plane of the frame, although the boundary condi-

I Professor, Disaster Prevention Research Institute, Kyoto University.
II Assistant, Disaster Prevention Research Institute, Kyoto University.
III Lecturer, Department of Architecture, Osaka Institute of Technology.
IV Graduate Student, Kyoto University. V Engineer, Naito Design Office.

tions of them are not the same strictly. (c) The effects of secondai bending on the behavior of braces due to the existence of another frame elements are not important. (d) Flange local buckling at both ends and mid-span initiated by lateral deflection induces the concentration of plastic deformation and causes fatigue cracks at these portions.

THEORETICAL STUDIES

Two types of theoretical analyses on the behavior of the bar subjected to repeated axial force were reported at the 5th WCEE, in Rome. Theory (I) treated a bar as one dimensional continuum based on the elastic-perfectly plastic theory. Theory (II) was developed on the basis of modified Shanley's model. The former was extended to investigate the behavior of the bar with various types of yield conditions and estimate the effects of elastic end restraints against rotation. The latter was extended to examine the effects of constraints of end displacement of a brace by the frame elements. From the analysis, the behavior of the brace rigidly connected to frame elements with ordinary dimensions could be approximated to that of clamped brace or that of equivalent simply supported brace with a half length. A numerical analysis which takes into account of the effects of partial yielding of a section and extension of yield zone in longitudinal direction using more realistic stress-strain relationship under cyclic loading was newly done to trace accurately the experimental load-displacement relationship and to supplement the lack of the experimental data under random loading process in the formulation of the loops.

MATHEMATICAL EXPRESSION OF HYSTERESIS LOOPS

The formulation procedure of the mathematical expression of hysteretic loops is presented here. The formulated loops should be applied to the brace in the range of slenderness ratio $30 \sim 150$ with rectangular or wide-flange cross section designed to buckle about its weak axis.

General Description of Hysteresis Loops The hysteresis loops of a single brace can be characterized to be composed of four stages shown in Fig. 3(a). Stage A : The bar is almost straight and load capacity is nearly equal to the yield load in pure tension. Stage B : The portion near the mid-span of the bar is yielding under combined stress in tension and bending. Stage C : The portion near the mid-span of the bar is yielding in compression and flexure. Stage D : Elastic unloading range. These properties are idealized by a pair of mechanism lines and linear elastic range in the model loop, as shown in Fig. 3(b). It is assumed that any compression or tension mechanism lines keep the prescribed shapes in whole process of repeated loading, and can be obtained by the translation of a standard compression or tension mechanism line in δ-axis direction, respectively. The slope of the elastic recovery line is determined from the assumption that $\delta_t/\delta_c = \delta_t'/\delta_c' = \text{const.}$ (see Fig. 3(d)). When the loading direction is reversed at point P on the tension yield line (Stage A), the point representing the response of a bar moves toward point 0 on the elastic recovery line with the slope identical to the initial one (Stage D). From point 0, the response point moves on the compression mechanism line (Stage C). Amount of the horizontal movement of the responce point on the compression mechanism line prescribes the translation of point P. When the loading direction is reversed at point 1 on the compression mechanism line the response point moves on the elastic recovery line toward point 2 from where it moves on the new tension mechanism line, specified by point P' (Stage B), while point 0 translates to its new position 0'. If the response point passes through point P', it moves on the tension yield line. On the other hand, if the loading direction is reversed at point 3 on the tension mechanism line, the response point moves on the

new compression mechanism line specified by point 0''' after passing through the elastic recovery line.

Determination of Compression Mechanism Line The post-buckling behavior of a simply supported bar with ideal I-section made of elastic-perfectly plastic material was derived as the following equation in Ref. 7).

$$\delta = n + (1 - n)(n_E - n)/(3n) + n_E(1 - n)^2/(6n^2)$$

n is expressed as the following form.

$$n = 1/\sqrt{6\delta/n_E + 1 + 2/n_E - 8/n_E}/\sqrt{6\delta/n_E + 1 + 2/n_E - 8/n_E}/\sqrt{}$$

Based on this equation the compression mechanism line for rectangular cross section is approximated to $n = 1/(a\cdot\delta + b)^{1/2}$. Fig. 4(a) shows $1/n^2$ vs. δ relations obtained from e aents. These relationships are approximated by straight lines and their slopes and intersections with the ordinate correspond to a and b, respectively. a and b are determined from Fig. 4(b).

$$n = 1/(a\cdot\delta + b)^{1/2} \ , \ a(n_E) = (10/n_E - 1)/3 \geq 0 \ , \ b(n_E) = 4/n_E + 0.6 \geq 1 \quad (1)$$

The formulated curves are compared with experimental ones, in Fig. 4(c).

Determination of Tension Mechanism Line The tension mechanism line is deliberately put in the same form as the compression mechanism line, $n = 1/(c\cdot\delta + d)^r$. Where d = 1 from the definition that the mechanism lines should pass through the normalized point (0,1) in Fig. 5(c). As shown in Fig. 5(a), $(1/n^{2/3}-1)$ vs. δ relation obtained from experimental tension mechanism lines are approximated to straight lines which pass through the origin. Coefficients c and r are determined from Fig. 5(b), as follows.

$$n = 1/(c\cdot\delta + 1)^r \ , \ r = 3/2 \ , \ c = 1/(3.1\, n_E + 1.4) \quad (2)$$

In Fig. 5(c), Eq. (2) is compared with experimental results.

Translation Rule of Mechanism Lines In Fig. 6(a), plotted are the translation x of the tension mechanism line under constant displacement amplitude δ_a versus the horizontal distance s between the latest characteristic point P and the load reversal point Q relations (see Fig. 3(c)). From the figure, it is understood that x-s relations are linear and the slope of the curves is independent of the displacement amplitude. From above-mentioned consideration, x is approximated to $x = \bar{x} - \eta\cdot s$, where $\eta = 0.115/n_E + 0.36$ from Fig. 6(b). $\bar{x}$ corresponding to the translation in the case of s = 0 is determined as the function of the plastic displacement amplitude $\bar{\delta}_a$ (see Fig.3(d)).

$$x = \ln(\zeta\cdot\bar{\delta}_a + 1) - \eta\cdot s \ , \quad \zeta = (3 - 1/n_E)/10 \quad (3)$$

The compression mechanism lines translate in such a manner that the condition $\delta_1'/\delta_2' = \delta_1/\delta_2$ is satisfied, in Fig. 3(b)

Elastic Recovery Line Figure 7(a) shows δ_t vs. δ_c relations (see Fig. 3 (a)) obtained from the experiments. The ratio $\xi = \delta_t/\delta_c$ is approximated to be independent of the displacement amplitude, and is derived from Fig. 7(b), as follows, $\xi = 0.3\sqrt{n_E} + 0.24 \geq 1$ (4)

The formulated loops illustrated in Figs. 8(a) and (b) approximate well the experimental behaviors shown in Figs. 8(c) and (d), respectively.

MATHEMATICAL EXPRESSION OF POST-BUCKLING CURVE UNDER MONOTONIC LOADING

In this section, derived is the mathematical expression for the post-buckling behavior of a brace under compressive axial force. The n vs. δ relationship is simplified to the same form as the one in the previous section, accompanied by three modification functions g_1, g_2 and g_3.

$$n = g_1 \cdot g_2 \cdot g_3 / (a' \cdot \delta + b')^{1/2} \leq 1$$

a' and b' for a brace with ideal I-section are given by the correlation for theoretical results in Ref. 7)

$$a'(n_E) = (1/n_E + 6)/(2n_E) \ , \quad (n_E) = 1 + 2/n_E$$

The function g_1 which estimates the accurate buckling strength is given that

$$g_1 = n_{cr}(n_E) \cdot \{a' \cdot n_{cr}(n_E) + b'\}^{1/2} \qquad (6)$$

using arbitrarily selected column-curve $n_{cr}(n_E)$. Simple expression of the junction function g_2 is given by

$$g_2 = (1/g_3 - 1/g_1) \cdot n_{cr}(n_E)/\delta + 1/g_1 \qquad (7)$$

The modification function g_3 to take into account of the effects of the shape of cross-section on the post-buckling behavior is given by the following equation as the approximation curve for the theoretical results in Refs. 6) and 9) (Fig. 10).

$$g_3 = 2\alpha \cdot (1 - \alpha) \cdot n_E/\delta + 0.6\alpha + 0.4 \leqq 1.5 \qquad (8)$$

Figure 11 shows the formulated post-buckling curves. In Fig. 12, the formulated curves are compared with the experimental results using the column curve specified by the AIJ design standard for steel structures.

CONCLUDING REMARKS

(1) Based on a great store of information from experimental and theoretical works on the elastic-plastic behaviors of steel braces under cyclic loading, formulated were the accurate mathematical expression of the post-buckling curves and the hysteresis loops which can be directly applied to the dynamic analysis or structural design of bracing system.
(2) The formulated loops in which the load capacity was expressed as the function of displacement were characterized by four basic equations; two mechanism lines and two hysteretic rules, when the slenderness n_E was settled.
(3) In the case of monotonic loading in compression, more accurate expression of post-buckling behavior was formulated for braces with various types of cross section. In this formula, the column curve(n_{cr}-n_E relation) which is appropriately selected as the needs of the case demands, can be adopted.
(4) The hysteresis loops and the post-buckling curves proposed for the single bracing system, can be easily applied to the design use of the double- or multi-bracing system using the superposition method.

REFERENCES

1) M. Wakabayashi, T. Nonaka, O. Koshiro and N. Yamamoto, "An Experiment on the Behavior of a Steel Bar under Repeated Axial Loading", Annuals, Disaster Prevention Research Institute, Kyoto University, No. 14A, pp. 371 - 381, 1971 (in Japanese).

2) M. Wakabayashi, T. Nonaka, T. Nakamura, S. Morino and N. Yoshida, "Experimental Studies on the Behavior of Steel Bars under Repeated Axial Loading, Part 1", Annuals, Disaster Prevention Research Institute, Kyoto University, No. 16B, pp. 113 - 125, 1973 (in Japanese).

3) M. Shibata, T. Nakamura, N. Yoshida, S. Morino, T. Nonaka and M. Wakabayashi, "Elastic-Plastic Behavior of Steel Braces under Repeated Axial Loading", Proc. of the 5th WCEE, pp. 845 - 848, Rome, 1973.

4) Prof. Wakabayashi's Lab. "Experimental Studies on the Eartnquake Resistant Properties of the Actual Braces", Report to the Building Research Institute, Ministry of Construction, Vol. 1 - 3, 1974 - 1976 (in Japanese).

5) T. Nonaka, "An Elastic-Plastic Analysis of a Bar under Repeated Axial Loading", Int. J. Solids Structures, Vol. 9, pp. 569 - 580, 1973, with erratum in No. 10.

6) M. Wakabayashi, T. Nonaka and N. Yoshida, "An Analysis of a Bar with End Restraints under Repeated Axial Loading", Abstracts, Annual Meeting of Kinki Branch of AIJ, pp. 197 - 200, 1976 (in Japanese).

7) M. Wakabayashi, T. Nonaka and M. Shibata, "Studies on the Post-Buckling Behavior of Braces, Part 1", Abstracts, Annual Meeting of Kinki Branch of AIJ, pp. 197 - 200, 1972 (in Japanese).

8) M. Wakabayashi, M. Shibata and H. Masuda, "An Elastic-Plastic Analysis of a Bar Subjected to End Displacement", Annuals, Disaster Prevention Research Institute, Kyoto University, No. 18B, pp. 143 - 154, 1974 (in Japanese).

9) M. Wakabayashi and M. Shibata, "Studies on the Post-Buckling Behavior of Braces, Part 4", Abstracts, Annual Meeting of Kinki Branch of AIJ, pp. 201 - 204, 1976 (in Japanese).

FIGURES

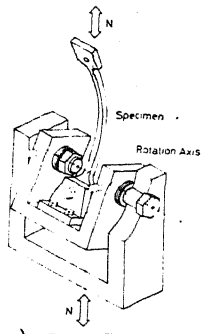

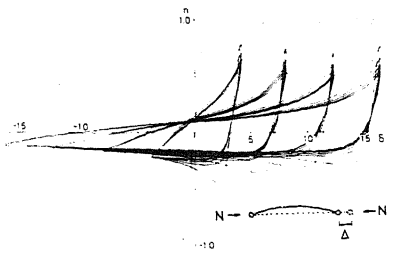

(a) End Support. (b) n_E = 1.13 (λ = 85).

Fig. 1 Test of Simply Supported Bar.

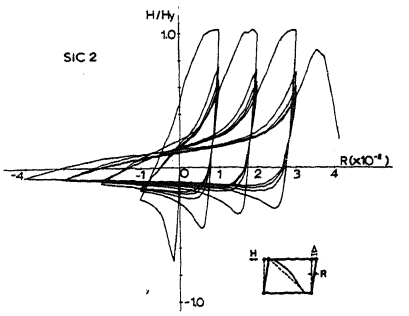

(c) Single Bracing System.

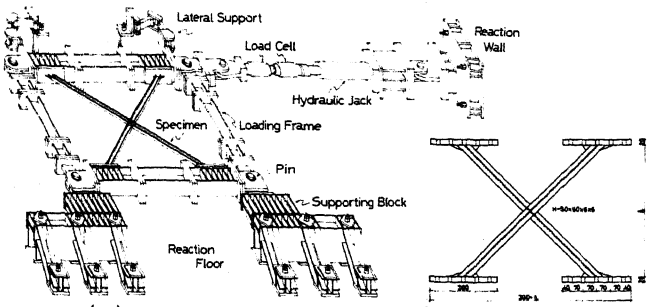

(a) Test Set Up. (b) Specimen.

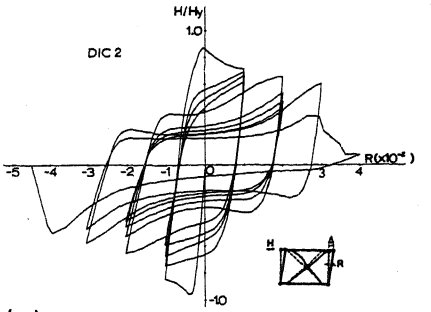

(d) Double Bracing System.

Fig. 2 Test of Wide Flange Brace.

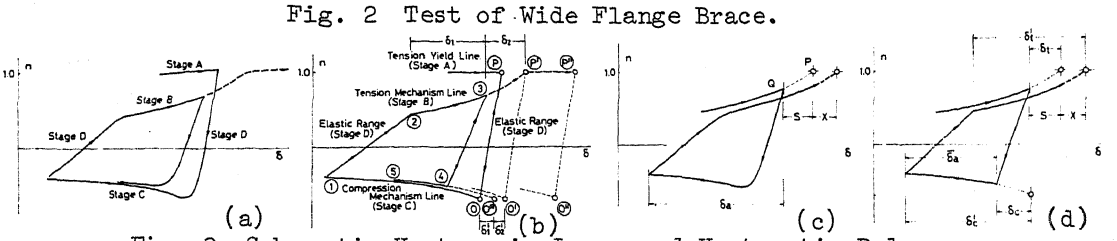

Fig. 3 Schematic Hysteresis Loops and Hysteretic Rules.

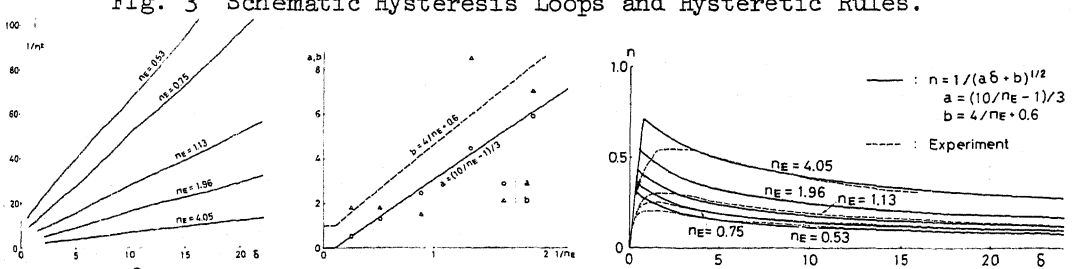

(a) $1/n^2$ vs. δ (b) a,b vs. n_E. (c) Formulated Curves.

Fig. 4 Formulation of Compression Mechanism Line.

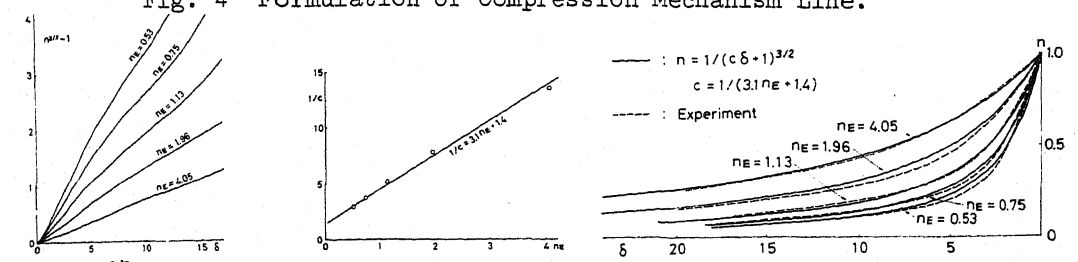

(a) $(1/n^{2/3} - 1)$ vs. δ. (b) 1/c vs. n_E. (c) Formulated Curves.

Fig. 5 Formulation of Tension Mechanism Line.

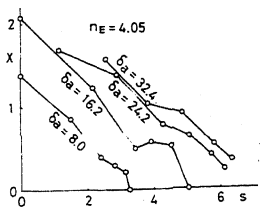

(a) x vs. s.

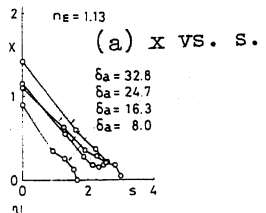

(b) η vs. n_E.

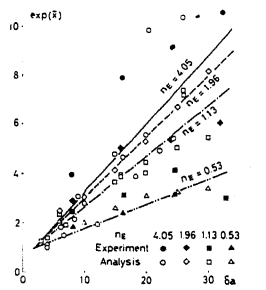

(c) $\text{Exp}(\bar{x})$ vs. δ_a.

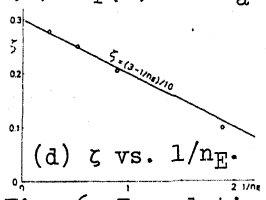

(d) ζ vs. $1/n_E$.

Fig. 6 Translation Rule of Tension Mechanism Line.

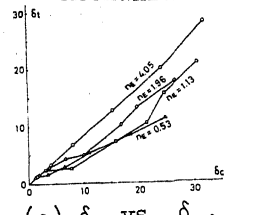

(a) δ_t vs. δ_c.

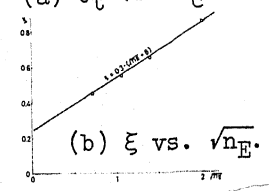

(b) ξ vs. $\sqrt{n_E}$.

Fig. 7 Elastic Recovery.

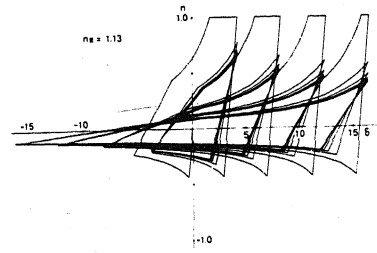

(a) Formulated Loop

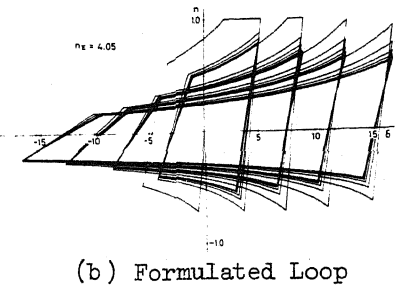

(b) Formulated Loop

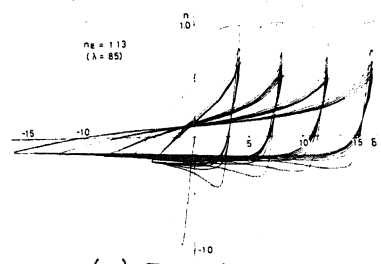

(c) Experiment.

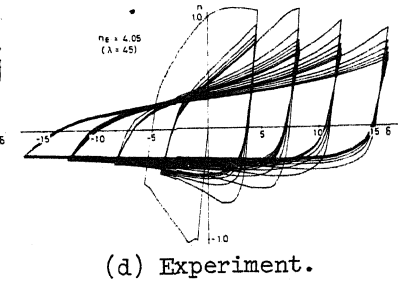

(d) Experiment.

Fig. 8 Comparison of Formulated Loops with Experiments.

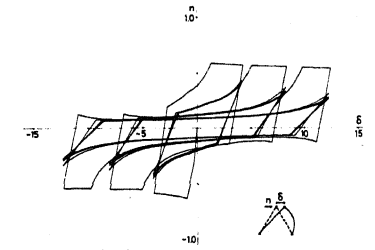

(a) $n_E = 0.53$

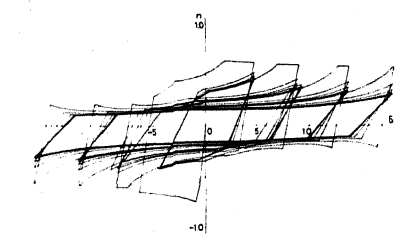

(b) $n_E = 1.96$

Fig. 9 Formulated Loops for Double Bracing System.

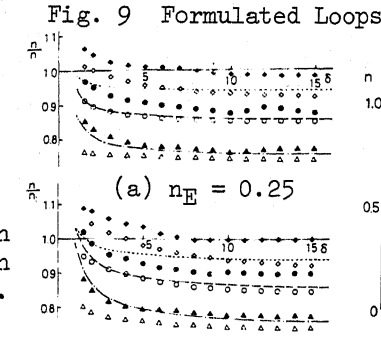

(a) $n_E = 0.25$

(b) $n_E = 0.5$

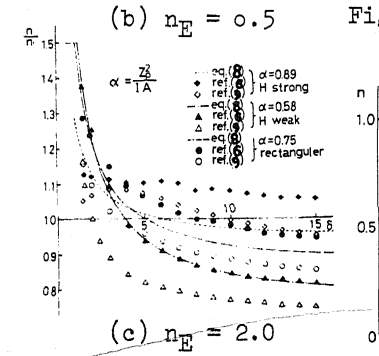

(c) $n_E = 2.0$

Fig. 10 Effects of Cross Sectional Shape.

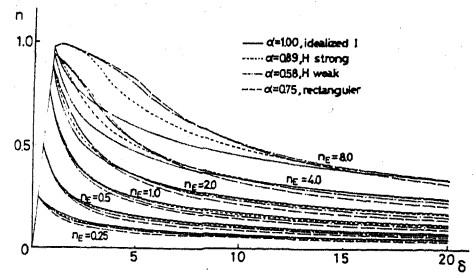

Fig. 11 Formulated Post-Buckling Curve.

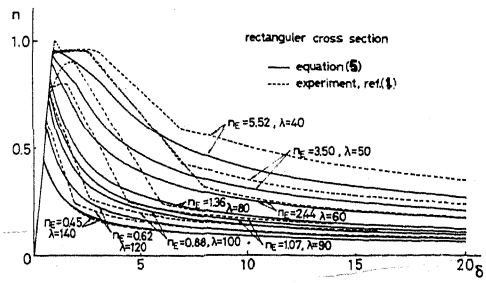

Fig. 12 Comparison of Formulated Curve with Experiment.

DISCUSSION

S.C. Goel (U.S.A.)

Would you elaborate on how your mathematical model accounts for the so-called "Column growth" phenomenon, i.e., the deterioration of tensile and compressive strength of a single brace under constant amplitude cyclic deformation ?

Author's Closure

With regard to the question of Mr. Goel, we wish to state that in the mathematical model, the deterioration of load carrying capacity in tension or compression range is prescribed by the translation x along the deformation axis (abscissa) of the tension or the compression mechanism line, respectively.

The compression mechanism line is a characteristic curve for the post-buckling behavior of a brace and the tension mechanism line is for the post-yielding behavior in the restretching range after buckling.

The translation x of the tension mechanism line is given by Eq. (3), using and s, where denotes the deformation amplitude on the latest compression mechanism line and s is a distance between the latest characteristic point P and the load reversal point Q on the tension mechanism line.

The coefficients and in Eq. (3) are determined by the parametric data analysis for experimental results (Fig.6).

On the other hand, the translation of the compression mechanism line is prescribed by the relation referring Fig. 3(b).